Available online at www.sciencedirect.com
ScienceDirect
Journal of the European Ceramic Society 27 (2007) 4265–4268
www.elsevier.com/locate/jeurceramsoc

EXAFS investigation on Sb incorporation effects to electrical transport in SnO_2 thin films deposited by sol–gel

V. Geraldo [a,b], V. Briois [c], L.V.A. Scalvi [a,*], C.V. Santilli [d]

[a] *Dep. Física FC, U. Estadual Paulista UNESP, C.P. 473, 17033-360 Bauru, SP, Brazil*
[b] *Instituto de Física de São Carlos-USP, C.P. 369, 13560-970 São Carlos, SP, Brazil*
[c] *Synchrotron SOLEIL, L'Orme des Merisiers, BP48, 91192 Gif-sur-Yvette, France*
[d] *I. Química, U. Estadual Paulista UNESP, C.P. 355, 14801-907 Araraquara, SP, Brazil*

Available online 21 March 2007

Abstract

The effect of Sb doping in SnO_2 thin films prepared by the sol–gel dip-coating (SGDC) process is investigated. Electronic and structural properties are evaluated through synchrotron radiation measurements by EXAFS and XANES. These data indicate that antimony is in the oxidation state Sb^{5+} and replaces tin atoms (Sn^{4+}), at a grain surface site. Although the substitution yields net free carrier concentration, the electrical conductivity is increased only slightly, because it is reduced by the high grain boundary scattering. The overall picture leads to a shortening of the grain boundary potential, where oxygen vacancies compensate for oxygen adsorbed species, decreasing the trapped charge at grain boundary.

Keywords: EXAFS; Tin dioxide films; Sol–gel

1. Introduction

In the undoped form, tin dioxide (SnO_2) is a wide bandgap n-type semiconductor, due to oxygen vacancies and interstitial tin atoms. When deposited as thin films, this material is characterized by high optical transmission in the ultraviolet (UV)–visible range and good electrical conductivity, being widely used as transparent electrodes in electronic devices.[1] SnO_2 thin film, deposited via sol–gel, is a polycrystalline combination of nanograins and the electrical properties may be controlled by the introduction of doping such as Sb^{5+} and the monitoring for oxygen adsorbed species on the surface and grain boundary.[2] Although doping with Sb^{5+} is an efficient process, this procedure is limited by the saturation, which takes place about 10 at% of Sb.[3] Besides, antimony presents variation of its oxidation state in the SnO_2 matrix (Sb^{5+} and/or Sb^{3+}), which may affect directly the electrical conductivity. If Sb^{5+} ions replace Sn^{4+} ions in a substitutional solid solution, they are supposed to act as donors in the SnO_2 matrix.

In this communication, SnO_2:Sb colloidal suspensions prepared by sol–gel route were used for thin film deposition by dip-coating technique. The variation of structural properties has been investigated by using synchrotron radiation, through XANES (X-ray absorption near edge structure) and EXAFS (extended X-ray absorption fine structure) measurements, in order to obtain information on Sb oxidation state as well as the effect of Sb doping in electrical transport properties of transparent SnO_2 films.

2. Experimental

Colloidal suspensions of Sb-doped SnO_2 have been prepared with an aqueous solution of Sn^{4+} (0.5 mol/l) obtained by dissolution of $SnCl_4{\cdot}5H_2O$, and an alcoholic solution of Sb obtained by dissolution of SbF_3. The nominal concentration of solutions range from 3.0 to 16.0 at% of Sb. Hydrolysis of Sn^{4+} and Sb^{3+} ions were promoted by addition of ammonium hydroxide (NH_4OH) under stirring with a magnetic bar until pH reaches 11. The suspension was submitted to dialyses against distilled water for elimination of chloride and fluoride ions. Films were deposited by dip-coating with 10 cm/min withdrawal rate, followed by drying in air by 20 min, and placed in a muffle at 200 °C by 30 min between each of the 10 layers. Then, samples were fired at 550 °C by 1 h.

XANES and EXAFS measurements were carried out at room temperature, at HASYLAB (HAmburg SYnchrotron radiation

* Corresponding author. Tel.: +55 14 3103 6084; fax: +55 14 3103 6094.
E-mail address: scalvi@fc.unesp.br (L.V.A. Scalvi).

0955-2219/$ – see front matter © 2007 Elsevier Ltd. All rights reserved.
doi:10.1016/j.jeurceramsoc.2007.02.137

LABoratory) (4.5 GeV, 140 mA) Germany. XANES measurements at Sb L_1 edge (4698 eV) were carried out on the E4 station, using as monochromator a Si (1 1 1) double crystal. The XANES data for films were recorded in total electron yield detection mode using the detector developed by Tourillon et al.[4] XANES spectra were normalized far from the edge (~4750 eV) and analyzed in comparison to Sb_2O_3 and $FeSbO_4$ references to determine the Sb oxidation in the Sb-doped SnO_2 thin films. EXAFS data were recorded at Sb K edge (30491 eV) and Sn K edge (29200 eV) of ROMO II station at HASYLAB, equipped with a Si (3 1 1) double crystal monochromator which was set to 60% in order to eliminate higher harmonics. Sn K edge data were recorded in transmission mode over 1200 eV with 2 eV energy steps. Sb K edge EXAFS spectra were measured in fluorescence mode using a solid state Ge monoelement detector over 1000 eV with 2 eV energy steps. Sn K edge EXAFS oscillations were analysed according to the procedure fully described elsewhere[5] using the EXAFS98 and ROUND Midnight programs[6].

For electrical measurements, In electrodes have been evaporated on the samples by an Edwards evaporator system and annealed to 150 °C by 20 min. Low temperature data were obtained in an Air Product Cryostat that controls temperature in the range 25–300 K within 0.05 K of precision.

3. Results–discussion

Fig. 1(a) shows a plot of electrical resistivity as function of Sb doping for several temperatures of SnO_2 thin films. The overall effect of doping is to decrease the resistivity as the concentration of Sb doping increases until the saturation is reached, which is about 10%.[3] Therefore, the sample with 9 at% of Sb presents the overall lower resistivity. However this resistivity is still high in comparison to films deposited by similar procedures.[1,7] These data raises several possibilities: (i) the doping is not being completely incorporated into the sample, (ii) the Sb doping is preferentially in the Sb^{3+} state, instead of Sb^{5+} (donor), giving birth to a high charge compensation and (iii) these films present a very low electron mobility.

L_1 Sb XANES data for Sb-doped films are compared in Fig. 1(b) with XANES data for reference compounds. In the Sb_2O_3 and the $FeSbO_4$ compounds, the antimony presents Sb^{3+} and Sb^{5+} oxidation sates, respectively. The spectra present maxima at 4703 and 4707 eV for Sb_2O_3 and $FeSbO_4$, respectively. Then the peak about 4707 eV, observed for Sb-doped film indicates an oxidation state of Sb^{5+}.[8]

XANES data obtained for thin films evidence the donor nature of Sb^{5+}, which rules out hypothesis (ii). Results of reflection in the near infrared[9] show that Drude's theory applies, which means a carrier concentration is as high as 10^{20} cm^{-3}. It assures that there is enough free electrons to lead to a highly degenerate semiconductor. All of these data lead us to investigate hypothesis (iii) carefully.

The influence of adding antimony to SnO_2 matrix was investigated by EXAFS at Sn K edge. The first peak ($1 < R < 2.2$ Å) of Fourier transform of EXAFS shown in Fig. 2(a) is related to the first oxygen coordination shell around tin atoms (Sn–O) and the second peak is related to Sn–Sn (3.19 Å), Sn–Sn (3.72 Å) and

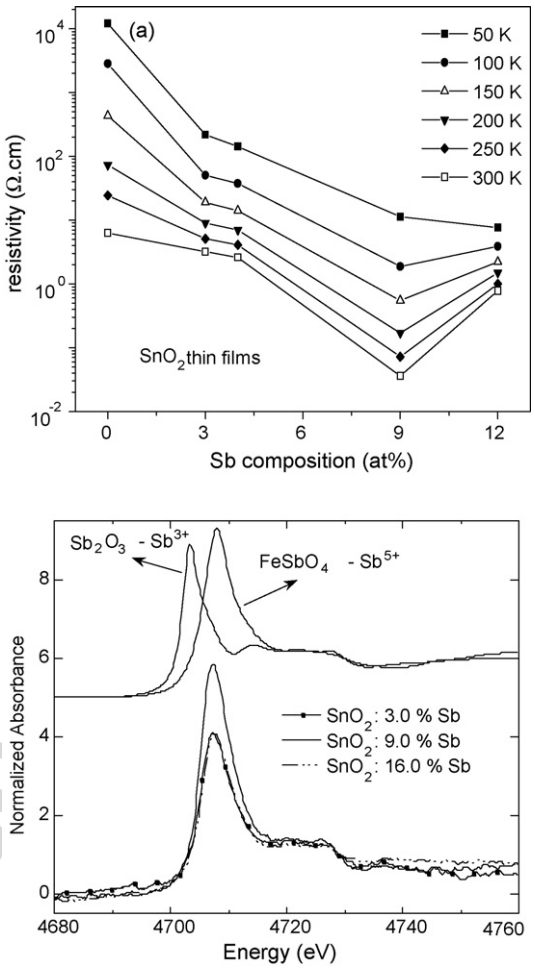

Fig. 1. (a) Resistivity as function of Sb doping in SnO_2 thin films, measured at several temperatures (lines are drawn only as a guide to the eyes). (b) XANES data for references compounds and Sb-doped SnO_2 thin films. Sb_2O_3 presents oxidation state Sb^{3+} and $FeSbO_4$, oxidation state Sb^{5+}.

Sn–O (3.58 Å) contributions of the second tin nearest neighbor. The decrease of the second peak for the films compared to the crystalline SnO_2 powdered reference is due to the nanometer scale of crystallites in the films. The smaller the crystallite, the fewer neighbors are present at the second coordination shell (Sn-Sn), and, thus, the second peak in the Fourier transform (FT) of EXAFS signal is lower. It can be noticed in Fig. 2(a) that the increase of antimony concentration does not change the intensity of the first oxygen contribution indicating that the first coordination shell of oxygen remains essentially invariant upon doping. Small differences in intensity can be observed in Fig. 2(a) for the second peak, in particular higher intensities are observed for the second maximum of this peak when Sb is added. This change can be related either to an increase of the crystallite size and/or to a decrease of the disorder inside the crystallite. In the latter case, it should be observed a decrease of the Debye–Waller factor.

Table 1 presents structural parameters obtained by a least-squares fitting procedure to simulate the first two peaks of the FT displayed in Fig. 2(a). It is clearly seen that the increase in the antimony concentration does not change the number of oxygen

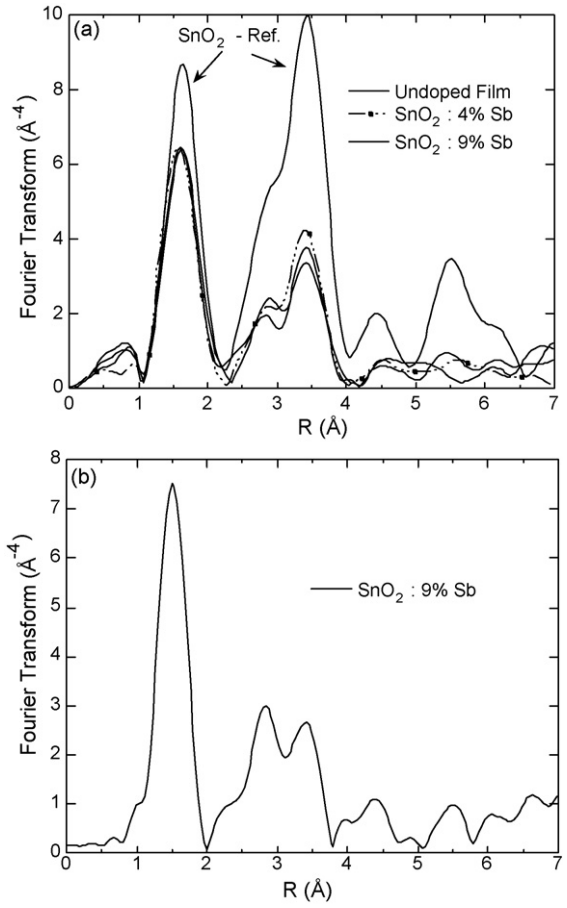

Fig. 2. (a) Fourier transforms of EXAFS signal at Sn K edge for films prepared with different Sb loadings compared to a crystalline SnO_2 reference. (b) Fourier transform of EXAFS signal at Sb K edge for SnO_2:9%Sb thin film.

of the first coordination shell of Sn. The overall effect of addition of antimony is an increase of the coordination numbers for the tin second neighbors located at 3.73 Å, the Debye–Waller factors for the tin contributions being essentially identical. This indicates that the addition of Sb gives rise to a small increase of the size of the SnO_2 crystallite. The error bar on the size estimated for larger crystallites from coordination numbers determined by EXAFS increases with the size of the crystallite, which means particle size is estimated as 5 ± 2 nm.

Fourier transform of EXAFS signal at Sb K edge for a 9%Sb-doped SnO_2 thin film is presented in Fig. 2(b). The very similar shape of FT obtained at both K edges for the same film suggests that Sb doping ions enter into the lattice substitutional to Sn atoms. Data fitting of Sb K edge EXAFS data for SnO_2:9%Sb can be summarized as follows: number of first oxygen neighbors: 5.0 ± 0.5, degree of disorder of the system (Debye–Waller factor): 0.09 ± 0.02 Å, distance between Sb–O atoms: 2.02 ± 0.02Å. It is noteworthy that the Sb-O distance in first coordination shell of doping is about 2% shorter than the Sn–O distance in the SnO_2 structure.

Using the procedure already used and described for Cu-doped xerogels[10], we have calculated by FeFF7 the theoretical EXAFS spectra of different possible substitutional sites for antimony in SnO_2 lattice taking into account the structural contraction of 3% for the first oxygen coordination shell around Sb. No contraction of distances has been considered for Sn and O atoms located at larger distances and the same Debye–Waller factor for all the paths involved in the considered cluster, equal to 0.07 Å, has been set. Fig. 3 compares the experimental signal of SnO_2:9%Sb film with theoretical EXAFS data when antimony gets into several distinct sites, substitutional to Sn^{4+} ions. The best agreement between experiment and theory for the $k\chi(k)$ signal is apparently obtained for Sb located at sites g and e.[10] Nevertheless the comparison of Fourier transforms of the

Table 1
Structural parameters determined from least-square fitting of the first two peaks of the Fourier transforms of EXAFS signal at Sn K edge in Fig. 2(a)

Sample	Number of neighbors N, and type	Debye–Waller factor, σ (Å)	Interatomic distance R (Å)	Agreement factor ρ (%)
Crystalline reference SnO_2	6 O	0.05	2.06	1.03
	2 Sn	0.04	3.21	
	8 Sn	0.05	3.74	
	4 O	0.20	3.57	
Undoped film	5.8 O	0.07	2.06	0.55
	1.7 Sn	0.06	3.21	
	5.9 Sn	0.08	3.74	
	4.0 0	0.18	3.65	
SnO_2:4%Sb	5.8 O	0.07	2.07	3.07
	1.7 Sn	0.06	3.22	
	6.5 Sn	0.08	3.75	
	4.0 O	0.12	3.63	
SnO_2:9%Sb	5.7 O	0.07	2.05	0.44
	1.8 Sn	0.07	3.20	
	6.3 Sn	0.08	3.72	
	4.0 O	0.16	3.59	

Accuracy in the determination is 10% for N, 20% for σ and 1% for R.

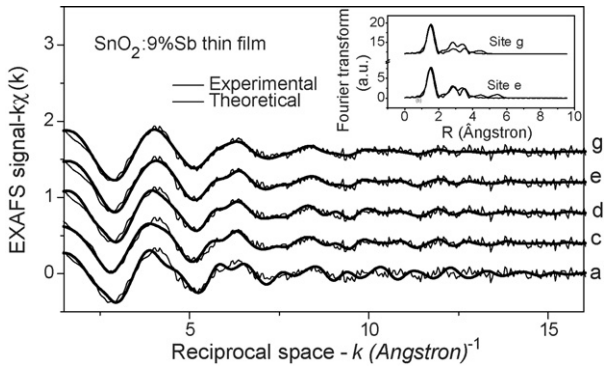

Fig. 3. (a) EXAFS signal at Sb K edge for SnO_2:9%Sb thin film, compared to theoretical calculation (FEFF program), according to Sb position at several distinct sites. Details on sites a, c–e and g can be found in Ref. [10]. *Inset*: Fourier transform of EXAFS signal and theoretical EXAFS by sites g and e.

$k\chi(k)$ signals for Sb impurity located at these two sites (g and e) undoubtedly addresses the site e (at cluster surface) as the best one. These results indicate that Sb enters into the lattice substitutional to Sn^{4+} and, moreover, the preferential site is located at grain surface. As concluded from XANES measurements (Fig. 2) the antimony presents +5 oxidation state in these films, providing the conclusion that Sb^{5+} substitutes Sn^{4+} in the SnO_2 lattice, yielding more free electrons and then, doping contribution is the improving of electrical conductivity. However, the calculation leading to Sb at an e-like site, located at the SnO_2 cluster surface, suggests also that besides substitutional position in the lattice, the impurity is also located preferentially close to grain surface. Finally it is important to stress that the substitution of Sn^{4+} by Sb^{5+} gives rise to oxygen vacancies inside the SnO_2 crystallites, which are located in the neighborhood of antimony since the average coordination of Sb is five-fold in spite of six-fold for Sn. The location of Sb close to the grain surface could explain that Sn K edge data are less sensitive to the presence of oxygen vacancies. But it appears from the Sb K edge data that Sb acts as a better probe in the SnO_2 crystallite to detect oxygen vacancy.

The picture drawn by the combination of results presented so far can be summarized as follow: highly doped SnO_2 thin films with nanoscopic grains present the doping in the Sb^{5+} oxidation state, which is located into the lattice substituting to Sn^{4+}, preferentially at grain boundary layer. In addition, the Sb doping leads to an increase in the oxygen vacancy concentration, what helps to improve the free carrier concentration. Considering only the charge carriers contribution, the sample should have its resistivity substantially decreased by the high doping. However this is not observed. This picture is consistent with very low electron mobility due to grain boundary scattering associated to the nanocopic grain size. Then, the slight increase in the conductivity with doping concentration is due to oxygen vacancies surrounding Sb^{5+} ions, located at grain boundary layer, since it compensates for the adsorbed species and the overall result is a decrease of the potential barrier, what increases the charge carrier mobility.

4. Conclusion

XANES data indicate that the antimony atoms are in the oxidation state +5. The *ab initio* simulation of experimental EXAFS at Sb K edge evidences the presence of antimony atoms in a substational site located at grain boundary surface region, which must influence the intergrain charge potential barrier. Besides, the increasing of Sb concentration also increases the oxygen vacancy concentration. Small grains imply in a higher amount of grains and higher grain boundary scattering, which means a very low mobility, even though the free carrier concentration is high. Film mobility is slightly increased due to Sb doping, related with lowering of grain boundary potential barrier, due to reducing trapped charge by interaction with oxygen vacancies. The general effect is to increase the film conductivity with Sb doping concentration.

Acknowledgments

The authors wish to thank Brazilian sources for financial help: CAPES, CNPq and FAPESP. DESY and the European Community is acknowledged for the financial support for the access to Hasylab (Contract RII3-CT-2004-50600, IA-SFS).

References

1. Hu, Y. and Hou, S. H., Preparation and characterization of Sb-doped SnO_2 thin films from colloidal precursors. *Math. Chem. Phys.*, 2004, **86**, 21–25.
2. Kololuoma, T. and Rantala, J. T., Effect of argon plasma treatment conductivity of sol–gel fabricated Sb-doped SnO_2 thin films. *Electron Lett.*, 2000, **36**, 172–173.
3. Nütz, T. and Haase, M., Wet-chemical synthesis of doped nanoparticles: Optical properties of oxygen-deficient and antimony-doped colloidal SnO_2. *J. Phys. Chem. B*, 2000, **104**, 8430–8437.
4. Tourillon, G., Dartyge, E., Fontaine, A., Lemonnier, M. and Bartol, F., Electron yield X-ray absorption-spectroscopy at atmospheric-pressure. *Phys. Lett. A*, 1987, **121**, 251–257.
5. Briois, V., Santilli, C. V., Pulcinelli, S. H. and Brito, G. E. S., EXAFS and XRD analysis of the structural evolutions involved during drying of SnO_2 hydrogels. *J. Non Cryst. Solids*, 1995, **191**, 17–28.
6. Michalowicz, A., EXAFS pour le Mac, Logiciels pour la Chimie. *Soc. Fr. Chim.*, 1991, 102–121.
7. Elangovan, E., Shivashankar, S. A. and Ramamurthi, K., Studies on structural and electrical properties of sprayed SnO_2:Sb films. *J. Cryst. Growth*, 2005, **276**, 215–221.
8. Millet, J. M. M., Baca, M., Pigamo, A., Vitry, D., Ueda, W. and Dubois, J. L., Study of the valence state and coordination of antimony in MoVSbO catalysts determined by XANES and EXAFS. *Appl. Catal. A: Gen.*, 2003, **244**, 359–370.
9. Shanthi, E., Dutta, V., Banerjee, A. and Chopra, K. L., Electrical and optical-properties of undoped and antimony-doped tin oxide-films. *J. Appl. Phys.*, 1980, **51**, 6243–6251.
10. Santilli, C. V., Pulcinelli, S. H., Brito, G. E. S. and Briois, V., Sintering and crystallite growth of nanocrystalline copper doped tin oxide. *J. Phys. Chem. B*, 1999, **103**, 2660–2667.